High spatial frequency periodic structures induced on metal surface by femtosecond laser pulses

Jian-Wu Yao,[1] Cheng-Yun Zhang,[1] Hai-Ying Liu,[1] Qiao-Feng Dai,[1] Li-Jun Wu,[1] Sheng Lan,[1,*] Achanta Venu Gopal,[2] Vyacheslav A. Trofimov,[3] and Tatiana M. Lysak[3]

[1]*Laboratory of Photonic Information Technology, School of Information and Optoelectronic Science and Engineering, South China Normal University, Guangzhou 510006, China*

[2]*Department of Condensed Matter Physics and Material Science, Tata Institute of Fundamental Research, Homi Bhabha Road, Mumbai 400005, India*

[3]*Department of Computational Mathematics and Cybernetics, M. V. Lomonosov Moscow State University, Moscow 119992, Russia*

**slan@scnu.edu.cn*

Abstract: The high spatial frequency periodic structures induced on metal surface by femtosecond laser pulses was investigated experimentally and numerically. It is suggested that the redistribution of the electric field on metal surface caused by the initially formed low spatial frequency periodic structures plays a crucial role in the creation of high spatial frequency periodic structures. The field intensity which is initially localized in the grooves becomes concentrated on the ridges in between the grooves when the depth of the grooves exceeds a critical value, leading to the ablation of the ridges in between the grooves and the formation of high spatial frequency periodic structures. The proposed formation process is supported by both the numerical simulations based on the finite-difference time-domain technique and the experimental results obtained on some metals such as stainless steel and nickel.

OCIS codes: (220.4241) Nanostructure fabrication; (350.3390) Laser materials processing; (160.3900) Metals.

References and links

1. M. Birnbaum, "Semiconductor surface damage produced by ruby lasers," J. Appl. Phys. **36**(11), 3688–3689 (1965).
2. P. M. Fauchet and A. E. Siegman, "Surface ripples on silicon and gallium arsenide under picosecond laser illumination," Appl. Phys. Lett. **40**(9), 824–826 (1982).
3. J. E. Sipe, J. F. Young, J. S. Preston, and H. M. Van Driel, "Laser-induced periodic surface structure. I. Theory," Phys. Rev. B **27**(2), 1141–1154 (1983).
4. J. S. Preston, H. M. van Driel, and J. E. Sipe, "Pattern formation during laser melting of silicon," Phys. Rev. B Condens. Matter **40**(6), 3942–3954 (1989).
5. S. E. Clark and D. C. Emmony, "Ultraviolet-laser-induced periodic surface structures," Phys. Rev. B Condens. Matter **40**(4), 2031–2041 (1989).
6. J. Reif, F. Costache, M. Henyk, and S. V. Pandelov, "Ripples revisited: nonclassical morphology at the bottom of femtosecond laser ablation craters in transparent dielectrics," Appl. Surf. Sci. **197–198**, 891–895 (2002).
7. R. Wagner, J. Gottmann, A. Horn, and E. W. Kreutz, "Subwavelength ripple formation induced by tightly focused femtosecond laser radiation," Appl. Surf. Sci. **252**(24), 8576–8579 (2006).
8. V. R. Bhardwaj, E. Simova, P. P. Rajeev, C. Hnatovsky, R. S. Taylor, D. M. Rayner, and P. B. Corkum, "Optically produced arrays of planar nanostructures inside fused silica," Phys. Rev. Lett. **96**(5), 057404 (2006).
9. J. Wang and C. Guo, "Ultrafast dynamics of femtosecond laser-induced periodic surface pattern formation on metals," Appl. Phys. Lett. **87**(25), 251914 (2005).
10. A. Y. Vorobyev and C. Guo, "Femtosecond laser-induced periodic surface structure formation on tungsten," J. Appl. Phys. **104**(6), 063523 (2008).
11. A. Borowiec and H. K. Haugen, "Subwavelength ripple formation on the surfaces of compound semiconductors irradiated with femtosecond laser pulses," Appl. Phys. Lett. **82**(25), 4462–4464 (2003).
12. R. Le Harzic, H. Schuck, D. Sauer, T. Anhut, I. Riemann, and K. König, "Sub-100 nm nanostructuring of silicon by ultrashort laser pulses," Opt. Express **13**(17), 6651–6656 (2005).

#157813 - $15.00 USD Received 9 Nov 2011; revised 27 Nov 2011; accepted 27 Nov 2011; published 4 Jan 2012

13. D. Dufft, A. Rosenfeld, S. K. Das, R. Grunwald, and J. Bonse, "Femtosecond laser-induced periodic surface structures revisited: a comparative study on ZnO," J. Appl. Phys. **105**(3), 034908 (2009).
14. L. Qi, K. Nishii, and Y. Namba, "Regular subwavelength surface structures induced by femtosecond laser pulses on stainless steel," Opt. Lett. **34**(12), 1846–1848 (2009).
15. X. Jia, T. Q. Jia, Y. Zhang, P. X. Xiong, D. H. Feng, Z. R. Sun, J. R. Qiu, and Z. Z. Xu, "Periodic nanoripples in the surface and subsurface layers in ZnO irradiated by femtosecond laser pulses," Opt. Lett. **35**(8), 1248–1250 (2010).
16. J. Wang and C. Guo, "Formation of extraordinarily uniform periodic structures on metals induced by femtosecond laser pulses," J. Appl. Phys. **100**(2), 023511 (2006).
17. J. Bonse, A. Rosenfeld, and J. Krüger, "On the role of surface plasmon polaritons in the formation of laser-induced periodic surface structures upon irradiation of silicon by femtosecond laser pulses," J. Appl. Phys. **106**(10), 104910 (2009).
18. M. Huang, F. Zhao, Y. Cheng, N. Xu, and Z. Xu, "Origin of laser-induced near-subwavelength ripples: interference between surface plasmons and incident laser," ACS Nano **3**(12), 4062–4070 (2009).
19. J. F. Young, J. S. Preston, H. M. van Driel, and J. E. Sipe, "Laser-induced periodic surface structures. II. Experiments on Ge, Si, Al, and brass," Phys. Rev. B **27**(2), 1155–1172 (1983).
20. F. Costache, M. Henyk, and J. Reif, "Modification of dielectric surfaces with ultra-short laser pulses," Appl. Surf. Sci. **186**(1-4), 352–357 (2002).
21. T. Q. Jia, H. X. Chen, M. Huang, F. L. Zhao, J. R. Qiu, R. X. Li, Z. Z. Xu, X. K. He, J. Zhang, and H. Kuroda, "Formation of nanogratings on the surface of a ZnSe crystal irradiated by femtosecond laser pulses," Phys. Rev. B **72**(12), 125429 (2005).
22. R. Le Harzic, D. Dörr, D. Sauer, F. Stracke, and H. Zimmermann, "Generation of high spatial frequency ripples on silicon under ultrashort laser pulses irradiation," Appl. Phys. Lett. **98**(21), 211905 (2011).
23. G. Miyaji and K. Miyazaki, "Origin of periodicity in nanostructuring on thin film surfaces ablated with femtosecond laser pulses," Opt. Express **16**(20), 16265–16271 (2008).
24. Y. Dong and P. Molian, "Coulomb explosion-induced formation of highly oriented nanoparticles on thin films of 3C–SiC by the femtosecond pulsed laser," Appl. Phys. Lett. **84**(1), 10–12 (2004).
25. G. Obara, N. Maeda, T. Miyanishi, M. Terakawa, N. N. Nedyalkov, and M. Obara, "Plasmonic and Mie scattering control of far-field interference for regular ripple formation on various material substrates," Opt. Express **19**(20), 19093–19103 (2011).
26. M. A. Ordal, L. L. Long, R. J. Bell, S. E. Bell, R. R. Bell, R. W. Alexander, Jr., and C. A. Ward, "Optical properties of the metals Al, Co, Cu, Au, Fe, Pb, Ni, Pd, Pt, Ag, Ti, and W in the infrared and far infrared," Appl. Opt. **22**(7), 1099–20 (1983).

1. Introduction

In the last two decades, laser induced periodic surface structures (LIPSSs) on the surfaces of various materials (including metals, semiconductors and dielectrics) with periods approximately equal to the laser wavelength have been investigated extensively by using nanosecond and picosecond lasers [1–5]. In recent years, this study has been extended to femtosecond (fs) lasers and it has been known that LIPSSs (e.g., ripples) can be created on the surface of a material when the laser fluence approaches the damage threshold of the material [6–15]. For different materials, the periods of LIPSSs induced by fs laser pulses are found to be smaller than laser wavelength. The interference between the incident laser light and the surface scattered wave was proposed many years ago to explain the formation of LIPSSs [3]. Recently, it is suggested that the surface plasmon polaritons (SPPs) excited by fs laser irradiation play a crucial role in the formation of LIPSSs [16–18]. In recent years, LIPSSs with periods significantly smaller than laser wavelength have attracted considerable interest because of their potential applications [11–15]. While the LIPSSs with periods approximately equal to the laser wavelength are called low spatial frequency LIPSSs (LSFLs), the LIPSSs with periods much smaller than the laser wavelength are referred to as high spatial frequency LIPSSs (HSFLs). Apparently, HSFLs induced by fs laser pulses cannot be interpreted by using the physical models described above [3,16–19]. So far, several mechanisms have been proposed to explain the formation of HSFLs induced by fs laser pulses, such as self-organization [20], second harmonic generation [11,21,22], excitation of SPPs [23], and Coulomb explosion [24] etc. However, the actual physical mechanism responsible for the generation of HSFLs is still debated. In addition, very few works related to the formation of HSFLs have been carried out on metals by using fs laser pulses. Very recently, the effects of various structures intentionally created on the surface on the fs laser ablation of material surface have been investigated. It clearly indicated that the structures created on the surface

#157813 - $15.00 USD Received 9 Nov 2011; revised 27 Nov 2011; accepted 27 Nov 2011; published 4 Jan 2012

would significantly influence the field intensity distribution on the surface and the subsequent ablation process [25].

In this article, we investigated experimentally and numerically the formation of HSFLs on metal surface by fs laser pulses. It is suggested that the redistribution of the electric field intensity due to the formation of LSFLs plays a crucial role in the creation of HSFLs. The proposed formation process of HSFLs is supported by both the numerical simulations based on the finite-difference time-domain (FDTD) technique and the experimental results obtained on metals such as stainless steel and nickel.

2. Experimental

In experiments, we used a Ti: sapphire fs amplifier (Legend, Coherent) that delivers 800 nm, 90 fs pulses at a repetition rate of 1 kHz. The metals we studied were 301 L stainless steel and nickel which are widely applied in industry. They were mechanically polished and cleaned in an ultrasonic cleaner with acetone. The surface roughness was less than 10 nm for the stainless steel sample and less than 3 nm for the nickel sample. The sample was fixed on a three-dimensional motorized translation stage. The horizontally polarized laser beam was focused normally on the sample by using a lens with a focusing length of 150 mm. A half-wave plate in combination with a polarizer was employed to control the laser ñuence. The diameter of the laser spot on the sample surface was measured to be ~40 μm. The laser scanning was carried out by translating the sample in the plane parallel to the sample surface. The surface morphology after fs laser ablation was examined by scanning electron microscope (SEM).

3. Results and discussion

3.1 HSFLs formed on metal surface

Recently, several research groups have reported the observation of HSFLs on different materials with periods much smaller than laser wavelength [11–15]. However, there are few reports on the formation of HSFLs on metals induced by fs laser pulses. In our experiments, we studied the formation and evolution of LIPSSs on metal surface by scanning fs laser beam across the metal surface with appropriate irradiation conditions. The scanning of laser beam ensures the uniform distribution of laser irradiation along the scanning line. Otherwise, the sample will be greatly ablated at the center of the ablation crater and HSFLs are only observed at the edge of the ablation crater [21]. It has been recognized that the morphology of LIPSSs depends strongly on the laser fluence and the number of irradiated pulses. Therefore, these two parameters were carefully controlled and adjusted. In our case, we fixed the laser fluence at 0.16 J/cm^2 which is slightly above the ablation threshold of the stainless steel. Then, the average number of fs laser pulses irradiated on the excitation spot was adjusted by varying the scanning speed of the laser beam from 2.0 to 0.25 mm/s. By doing so, the average number of fs laser pulses irradiated on the excitation spot ranges from 20 to 160. With these irradiation conditions, the surface of the stainless steel was processed by scanning the fs laser beam in the horizontal direction. The SEM images for the scanned lines obtained by using different scanning speeds are shown in Fig. 1. With a fast scanning speed of 2.0 mm/s, one can see a LSFL with a period of ~650 nm, as shown in Fig. 1(a). The LSFL consists of multiple grooves aligned in the horizontal direction. The formation of multiple grooves originates from the ripple-like electric field distribution on the surface. When the average number of irradiated pulses was increased to 40 (scanning speed = 1.0 mm/s), secondary grooves with a length of ~1 μm and a width of ~200 nm were created on the ridges of the primary grooves, as can be clearly seen in Fig. 1(b). With a further increase in the average number of irradiated pulses to 80 (scanning speed = 0.5 mm/s), it was found that the length of the primary grooves was almost doubled. In addition, it was noticed that the secondary grooves were significantly elongated and became equal to the primary grooves, as shown in Fig. 1(c). In this case, one cannot distinguish the primary grooves initially formed in the LSFL and the secondary grooves formed on the ridges of the primary ones. As a result, a

#157813 - $15.00 USD Received 9 Nov 2011; revised 27 Nov 2011; accepted 27 Nov 2011; published 4 Jan 2012

HSFL with a period equal to half of the LSFL was obtained. When the average number of irradiated pulses was increased to 160 (scanning speed = 0.25 mm/s), regular HSFL with a period of about 300 nm was created, as shown in Fig. 1(d).

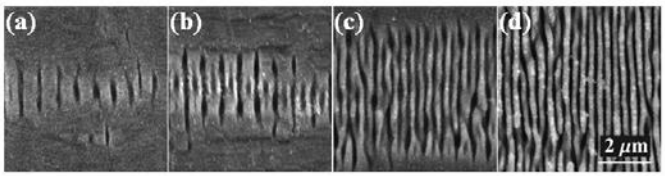

Fig. 1. SEM images of the scanned lines on the surface of stainless steel by using different scanning speeds: (a) 2.0 mm/s, (b) 1.0 mm/s, (c) 0.5 mm/s, and (d) 0.25 mm/s. The laser fluence was fixed at 0.16 J/cm^2.

Although LIPSSs have been studied extensively in the past, there is no report on the LIPSSs with secondary grooves sitting on the ridges of the primary grooves, as shown in Fig. 1(b). In fact, this kind of LIPSSs was observed not only on the surface of stainless steel but also on the surface of nickel. Figure 2 shows such a LIPSS formed on the surface of nickel by scanning fs laser beam with a fluence of 0.16 J/cm^2 and a scanning speed of 2.0 mm/s. The irradiation condition corresponds to an average number of irradiated pulses of 20 on the excitation spot. Under this condition, the length of the secondary grooves is slightly shorter than that of the primary ones. One can easily distinguish the initially and newly formed grooves. Therefore, the evolution of the LIPSS with increasing number of irradiated pulses clearly reveals a possible process for the generation of HSFLs, at least in some metals. As compared with the stainless steel, the formation of HSFLs was induced on the surface of nickel with a smaller average number of irradiated pulses. It is thought that the lager absorption coefficient of nickel at the laser wavelength is responsible for this behavior.

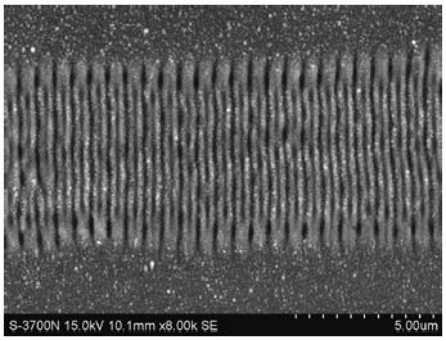

Fig. 2. SEM image of the LIPSS formed on the surface of nickel by scanning fs laser beam with a fluence of 0.16 J/cm^2 and a scanning speed of 2.0 mm/s.

3.2 Effect of LSFLs on the generation of HSFLs

As described at the beginning, several mechanisms have been proposed to explain the formation of HSFLs induced by fs laser pulses [11,20–24]. However, the actual mechanism of HSFL formation is still debated. It is thought that the physical mechanism for HSFL formation may depend strongly on the physical properties of materials. Different from semiconductors or dielectrics, metals are highly absorptive to laser light and the excitation of SPPs and localization of light may play an important role in the formation and evolution of LIPSSs. In fact, the interaction of the incident light with the metal surface will be modified after the formation of LSFLs, leading to the redistribution of the field intensity on the surface of metals. For shallow ripples (or grooves) formed on the surface of metals, it has been found that the incident light will be localized in the grooves, resulting in a deepening and an elongation of the grooves [18]. When the depth of the grooves exceeds a certain value,

#157813 - $15.00 USD Received 9 Nov 2011; revised 27 Nov 2011; accepted 27 Nov 2011; published 4 Jan 2012

however, it is expected that the distribution of electric field on the surface will be greatly changed, significantly affecting the subsequent ablation process. This behavior is confirmed by the numerical simulations described in the following.

3.3 Numerical simulation based on the FDTD technique

In order to gain a deep insight into the effect of LSFLs on the generation of HSFLs on metal surface, we have simulated the electric field distribution on the surface of a metal with initially formed ripples (or grooves) by using the FDTD technique. The simplified model for the structured surface used in our numerical simulation is schematically shown in Fig. 3. The V-shaped grooves created on the surface are described by four structural parameters *l*, *w*, *h*, and *d*, which denote the length, width, depth, and period of the grooves, respectively. Based on experimental observations and numerical simulations, it is found that the variations of *l*, *w*, and *d* may affect the electric field distribution in the grooves. However, the variations in these parameters do not induce obvious change in the electric field distribution on the surface of the metal. In other words, it is the depth of the grooves that plays an important role in the redistribution of the electric field or the formation of HSFLs. Based on experimental observation, we chose l = 6.0 μm, w = 0.2 μm, d = 0.65 μm and varied h to see its effect on the distribution of the electric field. In the numerical simulations, the Drude model is employed to describe the physical properties of metals. The real and imaginary parts of the dielectric constant of nickel at 800 nm are chosen to be $\varepsilon_r = -1.3$ and $\varepsilon_i = 2.17$, respectively [26]. The behavior of the stainless steel is expected to be similar to that of nickel because of the similar dielectric constant. Some typical simulation results are presented in Fig. 4.

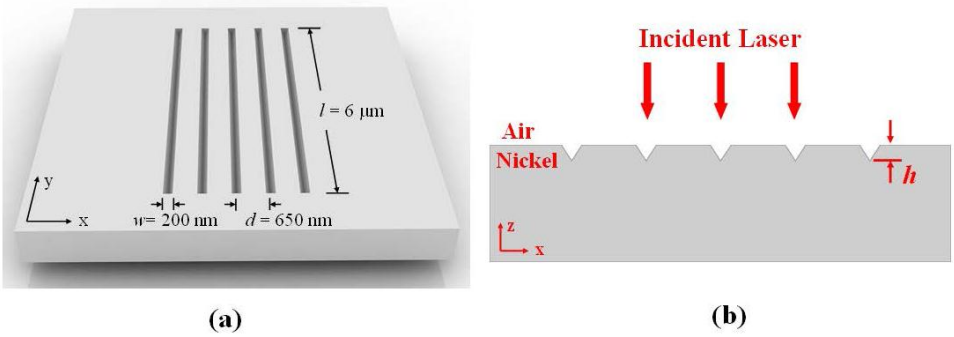

Fig. 3. Simplified model for the structured surface used in the numerical simulations.

For shallow grooves with h ~80 nm, the numerical simulation shows that the electric field is mainly localized in the grooves. This behavior has been reported previously [18]. It results in the deepening and elongation of the grooves. With a further increase of h to 150 nm, however, an obvious change is observed in the electric field distribution. One can easily find that the local maxima of the electric field occur on the ridges in between the two neighboring grooves. Although the field intensity of these maxima is still weaker than that localized in the grooves, they appear on the surface of the metal and affect the subsequent ablation of the surface. As expected, the intensities of these maxima increase with the deepening of the grooves, as shown in Figs. 4(c) and 4(d) for h = 200 and 300 nm, respectively. The intensities of these maxima even exceed the field intensities in the grooves for h = 300 nm. Once the field intensities of these maxima exceed the ablation threshold of the metal, shorter grooves will be created in between the initially formed grooves, as shown in Fig. 1(b). As a result, the incident light will be redistributed among the initially and newly formed grooves and some energy will be deposited on the newly formed grooves. This results in the deepening and elongation of the newly formed grooves. This process continues, leading to the formation of HSFLs, as shown in Figs. 1(c) and 1(d). When the depth of the grooves becomes larger, the field intensities in the grooves become weaker while those on the ridges become stronger. In

#157813 - $15.00 USD Received 9 Nov 2011; revised 27 Nov 2011; accepted 27 Nov 2011; published 4 Jan 2012

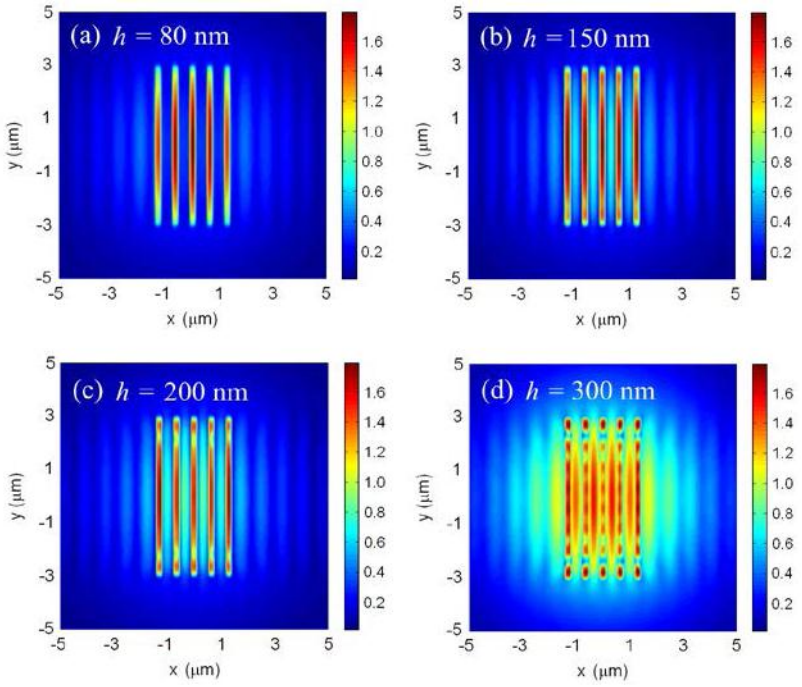

Fig. 4. Simulated electric field distribution on the surface of nickel (x-y plane) with grooves of different depths: (a) h = 80 nm, (b) h = 150 nm, (c) h = 200 nm, and (d) h = 300 nm.

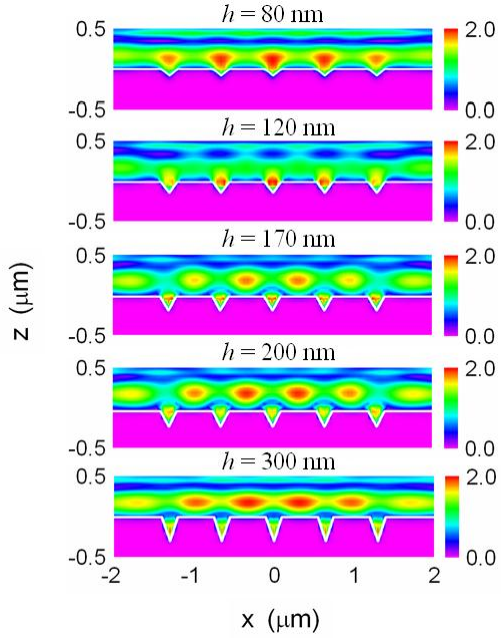

Fig. 5. Simulated electric field distributions in the x-z plane for grooves with different depths.

addition, the field distribution in the grooves is also changed, as shown in Figs. 4(a)–4(d). In Fig. 4(d), it is found that the separation between the local field maxima in the grooves is approximately equal to the laser wavelength (0.8 μm). Therefore, it is thought the deep grooves behave as plasmonic waveguides for light and the local field maxima originate from

#157813 - $15.00 USD Received 9 Nov 2011; revised 27 Nov 2011; accepted 27 Nov 2011; published 4 Jan 2012

the standing wave formed in the waveguides. We have also simulated the electric field distributions in the x-z plane for grooves with different depths. The simulation results shown in Fig. 5 reveal that the ablation of the grooves is alleviated and eventually stopped with the increase in the depth of the grooves. When h = 170 nm, the field intensity localized in the groves becomes weaker. For h > 200 nm, the field intensity is concentrated on the ridges in between the grooves, leading to the creation of new grooves. In addition, the field intensity in the initially formed grooves becomes very weak, implying that no ablation occurs in these grooves.

5. Conclusion

In summary, we have suggested a formation process for HSFLs on metal surface. Based on the FDTD simulation, it is revealed that the field intensity distribution on metal surface will be dramatically changed when the depth of the initially formed grooves exceeds a critical value. The field intensity which is localized in the grooves becomes concentrated on the ridges in between the grooves, leading to the creation of new grooves and thus the HSFLs. The proposed formation process was supported by the experimental results observed on stainless steel and nickel. It will be helpful for the fabrication and application of HSFLs on metal surface.

Acknowledgments

The authors acknowledge the financial support from the National Natural Science Foundation of China (Grant Nos. 10974060, 51171066 and 11111120068) and the project for high-level professionals in the universities of Guangdong province, China.

#157813 - $15.00 USD Received 9 Nov 2011; revised 27 Nov 2011; accepted 27 Nov 2011; published 4 Jan 2012